


# Post-translational cleavage of Hv1 in human sperm tunes pH- and voltage-dependent gating

Thomas K. Berger<sup>1,\*</sup> , David M. Fußhöller<sup>1,\*</sup>, Normann Goodwin<sup>1</sup>, Wolfgang Bönigk<sup>1</sup>, Astrid Müller<sup>1</sup>, Nasim Dokani Khesroshahi<sup>1</sup>, Christoph Brenker<sup>1,2</sup>, Dagmar Wachten<sup>4</sup>, Eberhard Krause<sup>3</sup>, U. Benjamin Kaupp<sup>1</sup> and Timo Strünker<sup>1,2</sup>

<sup>1</sup>Department of Molecular Sensory Systems, Center of Advanced European Studies and Research, Bonn, Germany

<sup>2</sup>Center of Reproductive Medicine and Andrology, University Hospital Münster, Münster, Germany

<sup>3</sup>Leibniz-Institute for Molecular Pharmacology, Berlin, Germany

<sup>4</sup>Max-Planck Research Group Molecular Physiology, Center of Advanced European Studies and Research, Bonn, Germany

## Key points

- In human sperm, proton flux across the membrane is controlled by the voltage-gated proton channel Hv1.
- We show that sperm harbour both Hv1 and an N-terminally cleaved isoform termed Hv1Sper.
- The pH-control of Hv1Sper and Hv1 is distinctively different.
- Hv1Sper and Hv1 can form heterodimers that combine features of both constituents.
- Cleavage and heterodimerization of Hv1 might represent an adaptation to the specific requirements of pH control in sperm.

**Abstract** In human sperm, the voltage-gated proton channel Hv1 controls the flux of protons across the flagellar membrane. Here, we show that sperm harbour Hv1 and a shorter isoform, termed Hv1Sper. Hv1Sper is generated from Hv1 by removal of 68 amino acids from the N-terminus by post-translational proteolytic cleavage. The pH-dependent gating of the channel isoforms is distinctly different. In both Hv1 and Hv1Sper, the conductance–voltage relationship is determined by the pH difference across the membrane ( $\Delta$ pH). However, simultaneous changes in intracellular and extracellular pH that leave  $\Delta$ pH constant strongly shift the activation curve of Hv1Sper but not that of Hv1, demonstrating that cleavage of the N-terminus tunes pH sensing in Hv1. Moreover, we show that Hv1 and Hv1Sper assemble as heterodimers that combine features of both constituents. We suggest that cleavage and heterodimerization of Hv1 represents an adaptation to the specific requirements of pH control in sperm.

(Received 28 July 2016; accepted after revision 8 November 2016; first published online 17 November 2016)

**Corresponding author** T. K. Berger: Department of Molecular Sensory Systems, Center of Advanced European Studies and Research, Ludwig-Erhard-Allee 2, 53175 Bonn, Germany. Email: thomas.berger@caesar.de

T. Strünker: Center of Reproductive Medicine and Andrology, Albert-Schweitzer-Campus 1, University Hospital Münster, 48149 Münster, Germany. Email: timo.struenker@ukmuenster.de

**Abbreviations**  $\Delta$ pH, pH difference across the membrane; GV, conductance–voltage relationship; HA, haemagglutinin A; HEK, human embryonic kidney; HTF, human tubular fluid; IDR, intrinsically disordered region; mPIC, mammalian protease inhibitor cocktail;  $M_w$ , molecular weight; MS, mass spectrometry; PD, pore domain;  $V_m$ , membrane potential; VSD, voltage-sensing domain.

\*These authors contributed equally to this work.

## Introduction

Protons ( $H^+$ ) are ubiquitous cellular messengers and their intracellular concentration ( $pH_i$ ) is regulated by intracellular buffers, active and passive proton transporters, and proton channels. In a variety of cell types, the voltage-gated proton channel Hv1 has been implicated in important physiological functions, including proton extrusion in lung epithelial cells (Iovannisci *et al.* 2010), regulation of pH homeostasis in phytoplankton (Taylor *et al.* 2011), B-lymphocyte signalling (Capasso *et al.* 2010), regulation of reactive oxygen production in immune cells (Henderson *et al.* 1987; Ramsey *et al.* 2009; El Chemaly *et al.* 2010), and maturation of human sperm (Lishko *et al.* 2010). Moreover, enhanced proton currents are associated with impaired recovery from ischaemic brain damage (Wu *et al.* 2012), a lower survival rate in patients suffering from breast cancer (Wang *et al.* 2012), and malignant B-lymphocytes (Hondares *et al.* 2014).

The Hv1 proton channel belongs to the superfamily of voltage-gated cation channels (Ramsey *et al.* 2006; Sasaki *et al.* 2006). Hv1 has been identified in various species across phyla, ranging from protists (Taylor *et al.* 2011), to tunicates (Sasaki *et al.* 2006), and to vertebrates (Ramsey *et al.* 2006). In 'classical' tetrameric voltage-gated cation channels, such as voltage-gated  $K^+$ ,  $Na^+$ , and  $Ca^{2+}$  channels, each subunit usually harbours six transmembrane segments (S1–S6) that fold into a voltage-sensing domain (VSD) and a pore domain (PD). The VSD and the PD encompass transmembrane segments S1–S4 and S5–S6, respectively. By contrast, Hv1 harbours a prototypical VSD domain but lacks a genuine PD. Reconstituted Hv1 protein is functional, demonstrating that the VSD encompasses the pore (Lee *et al.* 2008); two amino acid residues have been identified that affect proton selectivity, which provided clues about the proton permeation pathway (Berger and Isacoff 2011; Musset *et al.* 2011). Hv1 forms dimers (Koch *et al.* 2008; Lee *et al.* 2008; Tombola *et al.* 2008) and each subunit contains its own pore (Tombola *et al.* 2008).

Unlike any other member of that channel superfamily, activation of Hv1 depends in a characteristic fashion on the membrane voltage ( $V_m$ ) and the pH difference ( $\Delta pH = pH_o - pH_i$ ) across the membrane (Cherny *et al.* 1995): at  $\Delta pH = 0$ , Hv1 commences to open at +10 to +30 mV, whereas, at  $\Delta pH > 0$  and  $< 0$ , the activation curve is shifted by  $\sim 40$  mV/ $\Delta pH$  unit to more negative and positive potentials, respectively. However, changes in  $pH_i$  and  $pH_o$  that leave  $\Delta pH$  constant do not affect the voltage dependence of activation (Cherny *et al.* 1995). Thus, Hv1 senses  $\Delta pH$  rather than  $pH_i$  or  $pH_o$  itself. Consequently, Hv1 opens only at  $V_m$  values positive to the Nernst potential for protons, i.e. Hv1 carries only proton outward currents. In functional terms, the control of Hv1 by this unique coupling between  $\Delta pH$  and  $V_m$

represents a mechanism for curtailing excessive cytosolic acidification, e.g. during production of reactive oxygen species in macrophages (El Chemaly *et al.* 2010). However, the mechanisms underlying  $\Delta pH$  sensing and its coupling to voltage activation are unknown.

Here, we show that human sperm harbour an N-terminally cleaved Hv1 isoform, termed Hv1Sper. Hv1Sper is controlled not only by  $\Delta pH$ , but also by pH itself. Thus, Hv1Sper senses both  $\Delta pH$  and pH. Hv1Sper and Hv1 form heterodimers whose gating properties are different from those of the respective homodimers. The pH-dependent gating of Hv1Sper and Hv1Sper/Hv1 heterodimers might be a specialization of the channel to cope with the ever changing environments that sperm encounter during their journey across the female reproductive tract.

## Methods

### Ethical approval

The studies involving human material were performed in agreement with the standards set by the *Declaration of Helsinki*. Samples of human semen were obtained from healthy volunteers with their prior written consent. Approval of the ethic committee of the medical association Westfalen-Lippe and the medical faculty of the University of Münster: 4INie. Human lung epithelium was provided by Professor H. Schorle (University Hospital Bonn, Germany). Approval of the ethic committee of medical faculty of the University of Bonn: 036/08. Human testis lysates were provided by Professor R. Middendorff (University of Gießen, Germany). Approval of the ethic committee of the medical association Hamburg: OB.89. Ejaculated boar sperm were purchased from the GFS-Genossenschaft zur Förderung der Schweinehaltung eG (Ascheberg, Germany). Mouse epididymis were obtained from C57Bl/6N mice that were anaesthetized with isoflurane (Abbvie Deutschland, Ludwigshafen, Germany) and killed by cervical dislocation according to the German law of animal protection and the district veterinary office. *Xenopus laevis* frog oocytes were provided by C. Volk (Bonn-Rhein-Sieg University of Applied Sciences, Sankt Augustin, Germany) or purchased from Ecocyte (Castrop-Rauxel, Germany).

### Sample preparation

Ejaculates were liquefied at room temperature (RT) for 30–60 min. Motile sperm were purified by 'swim-up' in human tubular fluid (HTF) containing (in mM): 97.8 NaCl, 4.7 KCl, 0.2  $MgSO_4$ , 0.37  $KH_2PO_4$ , 2  $CaCl_2$ , 0.33 Na-pyruvate, 21.4 Na-lactic acid, 2.8 glucose and 21 HEPES, adjusted to pH 7.35 with NaOH. Motile sperm were washed twice with HTF by centrifugation (20 min at

700 gat RT). Sperm number was determined in a Neubauer cell counter. For electrophysiological recordings, human serum albumin (HSA, 3 mg ml<sup>-1</sup>; Irvine Scientific, Santa Ana, CA, USA) was added after washing. For capacitation, sperm were incubated in HTF containing 25 mM HCO<sub>3</sub><sup>-</sup> and HSA for ≥2 h (Brenker *et al.* 2012). For a subset of experiments (Fig. 3G and H), sperm subpopulations were separated. Accordingly, ~1.5 ml of ejaculate was layered on top of a density gradient of two liquid phases (PureSperm, Nidacon, Mölndal, Sweden) and centrifuged in accordance with the manufacturer's instructions. Highly motile sperm settled in the bottom fraction (200 μl) and in the pellet. Motile sperm were collected from the lower liquid phase (~1 ml). Immotile sperm were collected from the interface between lower and upper liquid phase (~800 μl). Mouse sperm were prepared from the epididymis by incision of the cauda followed by swim-out (15–30 min at 37 °C) in (mM): 135 NaCl, 4.8 KCl, 2 CaCl<sub>2</sub>, 1.2 KH<sub>2</sub>PO<sub>4</sub>, 1 MgSO<sub>4</sub>, 5.6 glucose, 0.5 Na-pyruvate, 10 L-lactate, and 10 HEPES, pH 7.4 with HCl.

### Protein purification

Proteins were purified from human sperm either directly after swim-up or after thawing of swim-up sperm pellets stored at -80°C. Whole-sperm proteins (Figs 1A and B, 2, 3A, E, and F, and 4C) were prepared by lysis of sperm in buffer A (in mM: 10 HEPES, 2 EGTA and 1 dithiothreitol, pH 7.4, with NaOH; 1 × 10<sup>7</sup> sperm/100 μl). After incubation on ice for 10 min, the samples were sonicated (three times for 30 s; Sonifier 450; Branson, Danbury, CT, USA) and triturated with a 22 G syringe needle. Subsequently, 10 × PBS (1 × PBS containing in mM: 130 NaCl, 7 Na<sub>2</sub>HPO<sub>4</sub>, and 3 NaH<sub>2</sub>PO<sub>4</sub>, adjusted to pH 7.4) was added to produce an isotonic solution. For SDS-PAGE analysis, the sample was supplemented with 4 × SDS loading buffer (200 mM TRIS, 8% SDS, 50% glycerol, 4% β-mercaptoethanol, 0.04% bromophenol blue, pH 6.8, with HCl). Membrane proteins from sperm (Figs 3C and G, 4D and 6B) were prepared by suspending the sperm in buffer B (in mM: 100 NaCl, 25 HEPES, pH 7.5, with NaOH; 1–3 × 10<sup>7</sup> sperm/50 μl). The samples were sonicated (three times for 30 s) and supplemented with 0.5% SDS (10 min tumbling at 4°C). Subsequently, the samples were centrifuged at 186 000 g at 4°C for 15 min. The supernatant was collected and cross-linked (see below) or directly supplemented with 4 × SDS loading buffer.

Human embryonic kidney (HEK) 293 cells were washed in PBS, pelleted by centrifugation (10 000 g for 5 min), lysed with lysis buffer A, and triturated with a syringe. Cells were incubated for 15 min on ice to allow hypotonic lysis. The cell suspension was centrifuged (100 000 g for 30 min) to separate the membrane from the soluble protein fraction. The supernatant was discarded and the

pellet was resuspended in 0.5 ml of PBS with 2 μl of mammalian protease inhibitor cocktail (mPIC). The protein concentration was determined using the Pierce BCA assay (Thermo Fisher Scientific Inc., Waltham, MA, USA). For SDS-PAGE analysis, 80 μl of 4 × SDS loading buffer was added.

Frog oocytes (20–40) were mechanically devitellinated under a stereoscope, washed twice with 1 ml of PBS, and homogenized in 1 ml of oocyte lysis buffer (in mM: 50 Na-phosphate, 150 NaCl and 10 KCl, pH 7.2, with NaOH) with 10 μl of mPIC by triturating with a 20 G needle, followed by a 27 G needle. The homogenized sample was centrifuged twice at 300 g for 10 min to remove the egg yolk. The cell suspension was then centrifuged (186 000 g for 30 min) and the pellet was stored at -80°C. If not noted otherwise, samples were maintained at 4°C during preparation.

### Western blotting

The samples were subjected to SDS-PAGE using 3–5% stacking gel and 12.5% separation gel, transferred onto polyvinylidene fluoride membrane, and probed with anti-Hv1 anti-FLAG, or anti-haemagglutinin A (HA) antibodies. The polyclonal antibody against the C-terminus of Hv1 (amino acids 248–262) was generated by Peptide Specialty Laboratories (Heidelberg, Germany). The anti-FLAG and anti-HA antibodies were purchased from Roche (Basel, Switzerland).

### Generation of Hv1Sper-HA from heterologous Hv1-HA

To test whether Hv1Sper is generated from full-length Hv1 protein by a sperm protease, heterologous Hv1, tagged at its C-terminus with the HA-tag, was incubated with whole sperm lysate. Sperm proteins were prepared as described above. 10 μg of heterologous Hv1-HA was incubated with whole-sperm protein from 3 × 10<sup>6</sup> sperm (unless otherwise specified) in 200 μl of buffer A at 4°C for 1 h. Subsequently, the sample was centrifuged (10 000 g at 4°C for 10 min) and resuspended in sample buffer.

### Chemical cross-linking

Heterologously expressed Hv1-FLAG and Hv1Sper-HA were prepared from frog oocytes as described above and cross-linked by incubation in buffer B including 300 μM CuSO<sub>4</sub> and 900 μM phenanthroline at RT for 1 h. The reaction was quenched using 7 mM EDTA and 2.8 mM N-ethylmaleimide (final concentration). Sperm-membrane proteins from human and boar were prepared as described above and cross-linked using the same cross-linker concentrations.

## Mass spectrometry (MS)

Following SDS-PAGE, protein bands were stained with Coomassie blue and cut from the gel; slices were destained and cut into small pieces ( $\sim 1 \text{ mm}^2$ ). After tryptic protein digestion, liquid chromatography and tandem-MS analysis were performed as described previously (Strünker *et al.* 2006).

## DNA constructs and expression in HEK293 cells and *Xenopus* oocytes

DNA constructs were cloned and sequenced using standard techniques. Hv1 (accession number AAH32672) tagged at its C-terminus with an HA-tag was subcloned into the pcDNA3.1 vector. HEK293 cells were transfected using the  $\text{Ca}^{2+}$ -phosphate method. Expression of Hv1 with a C-terminal FLAG-tag, and of Hv1- $\Delta$ 68

(i.e. Hv1Sper) with a C-terminal HA tag in *X. laevis* oocytes was achieved with the pGEMHE vector. Tandem constructs of Hv1Sper and Hv1 contained a 17 amino acid linker (GGSGGSGGSGGSGGSGG) (Tombola *et al.* 2008). The vector was linearized with *NheI* and transcribed using the T7 mMessage mMachine kit (Ambion, Austin, TX, USA). *Xenopus* oocytes were injected with 50 nl of RNA ( $0.25\text{--}1.25 \mu\text{g } \mu\text{l}^{-1}$ ) and incubated at  $14\text{--}16^\circ\text{C}$  for 1–5 days in ND96 medium containing (in mM): 96 NaCl, 2 KCl, 1.8  $\text{CaCl}_2$ , 1  $\text{MgCl}_2$ , 10 HEPES, 5 Na-pyruvate, and  $100 \text{ mg l}^{-1}$  gentamicin, adjusted to pH 7.5 with NaOH.

## Electrophysiological recordings and data analysis

Oocytes were mechanically devitellinated under a stereoscope and placed in a recording chamber under an inverted IX71 microscope (Olympus, Tokyo, Japan) equipped with a 20x objective. Patch electrodes were

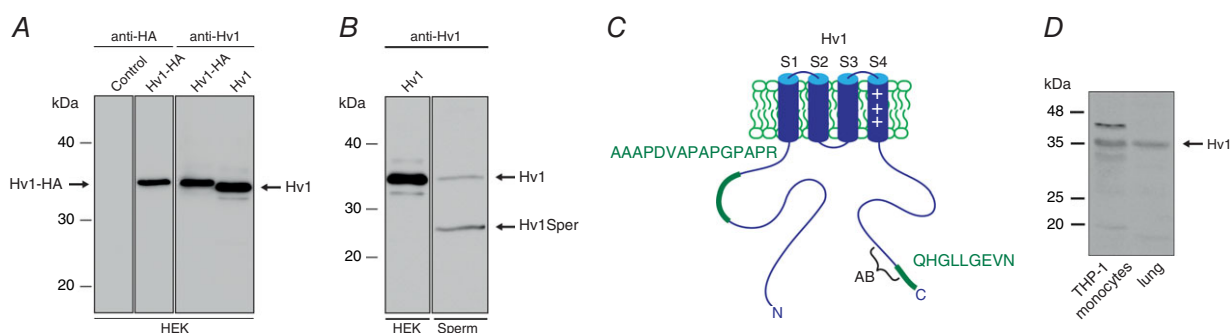


**Figure 1. Human sperm harbour full-length Hv1 and a short Hv1 variant**

**A**, western blot of HEK cells heterologously expressing Hv1-HA or Hv1, probed with a C-terminal anti-Hv1 or an anti-HA antibody. **B**, western blot of HEK cells expressing Hv1 and of human sperm, probed with a C-terminal anti-Hv1 antibody; in sperm, the antibody recognizes an additional protein of  $\sim 25 \text{ kDa}$  (termed Hv1Sper). **C**, cartoon of Hv1 showing the proteotypic peptides detected by MS (green) and the epitope of the anti-Hv1 antibody (AB). **D**, western blot of human monocyte cell line THP-1 and human lung epithelial cell lysate, probed with the C-terminal anti-Hv1 antibody.

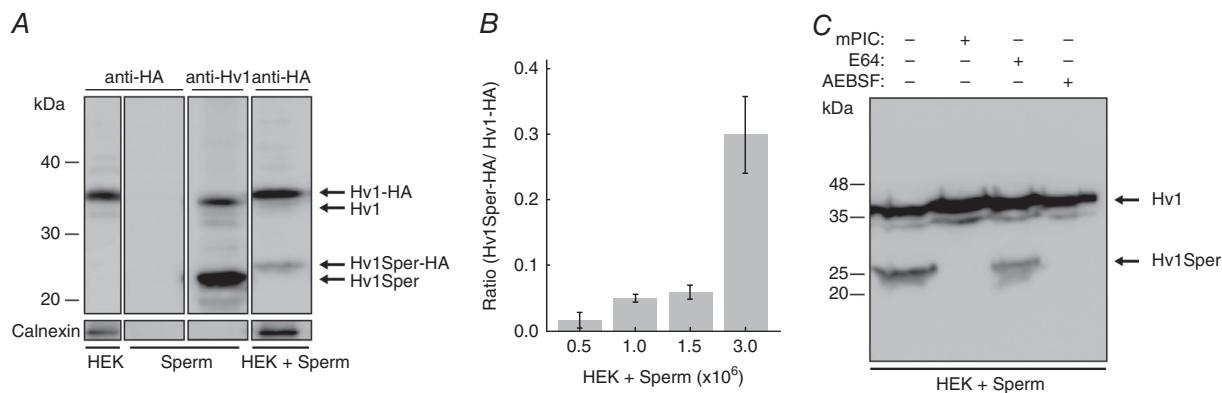


**Figure 2. Hv1 is post-translationally cleaved by a protease**

**A**, western blot of HEK cells expressing Hv1-HA, of human sperm, and of a mix of sperm and Hv1-HA-expressing HEK cells, probed with a C-terminal anti-Hv1 or an anti-HA antibody. **B**, Hv1Sper-HA/Hv1-HA band intensity is dependent on the ratio of the number of sperm in the sperm/HEK cell mix. **C**, western blot of a mix of sperm and Hv1-HA-expressing HEK cells in the presence or absence of protease inhibitors mPIC, E64, and AEBSF, as probed with an anti-HA antibody. Error bars indicate the SD.



pulled from borosilicate glass capillaries (Hilgenberg, Malsfeld, Germany) on a DMZ puller (Zeitz Instruments GmbH, Martinsried, Germany) and fire polished with a Narishige MF-830 microforge (Narishige, Tokyo, Japan), resulting in an initial electrode resistance of 0.7–1.5 M $\Omega$  (10–20  $\mu$ m inner tip diameter). Excised macropatches in the inside-out configuration were obtained within seconds to minutes. Holding potentials were –60 mV or –80 mV. Recordings were performed at room temperature (22–25°C) with an Axopatch 200B amplifier (Molecular Devices, Union City, CA, USA), connected via a Digidata 1440A acquisition board to pClamp 10 (Molecular Devices). Data were filtered at 2 or 5 kHz and the sampling rate was 10 kHz. Pipette (extracellular) and bath (intracellular) solutions contained (in mM): 100 HEPES, 30 methanesulphonic acid, 5 tetraethylammonium chloride, and 5 EGTA, adjusted to pH 7 with TEA hydroxide (>25 mM). HEPES was replaced by TRIS and 2-(N-morpholino) ethanesulphonic acid (MES) for solutions adjusted to pH 8 and 6, respectively. Data were analysed with Igor Pro (Wavemetrics, Portland, OR, USA). Tail currents for conductance–voltage relationship (GV)

recording were measured 5–25 ms after the end of the depolarizing voltage step. GV were fitted with a single Boltzmann function. For electrophysiological recordings of human sperm, cover slips (diameter 5 mm, thickness #1) were coated with poly-L-lysine and immersed in standard extracellular solution (HS), containing (in mM): 135 NaCl, 5 KCl, 1 MgSO<sub>4</sub>, 2 CaCl<sub>2</sub>, 5 glucose, 1 Na-pyruvate, 10 lactose, and 20 HEPES, adjusted to pH 7.4 with NaOH. Sperm in HTF solution were carefully pipetted onto a cover slip and allowed to settle for approximately 3 min. The cover slip was transferred to the recording chamber under an inverted microscope (IX71) equipped with a 60x NA 1.2 objective (UPLANSAPO; Olympus). Sperm currents were recorded under voltage clamp in the whole-cell configuration (Strünker *et al.* 2011). Seals between the patch pipette (initial resistance of 20–30 M $\Omega$ ) and the sperm cytoplasmic droplet were formed in HS solution. Extra- and intracellular recording solutions lacked alkali metal ions but contained high pH-buffer concentrations (in mM): 135 *N*-methyl-D-glucamine, 5 EGTA, and 100 HEPES or MES, adjusted with methanesulphonic acid to pH 7 or 6, respectively. Chemicals were purchased from

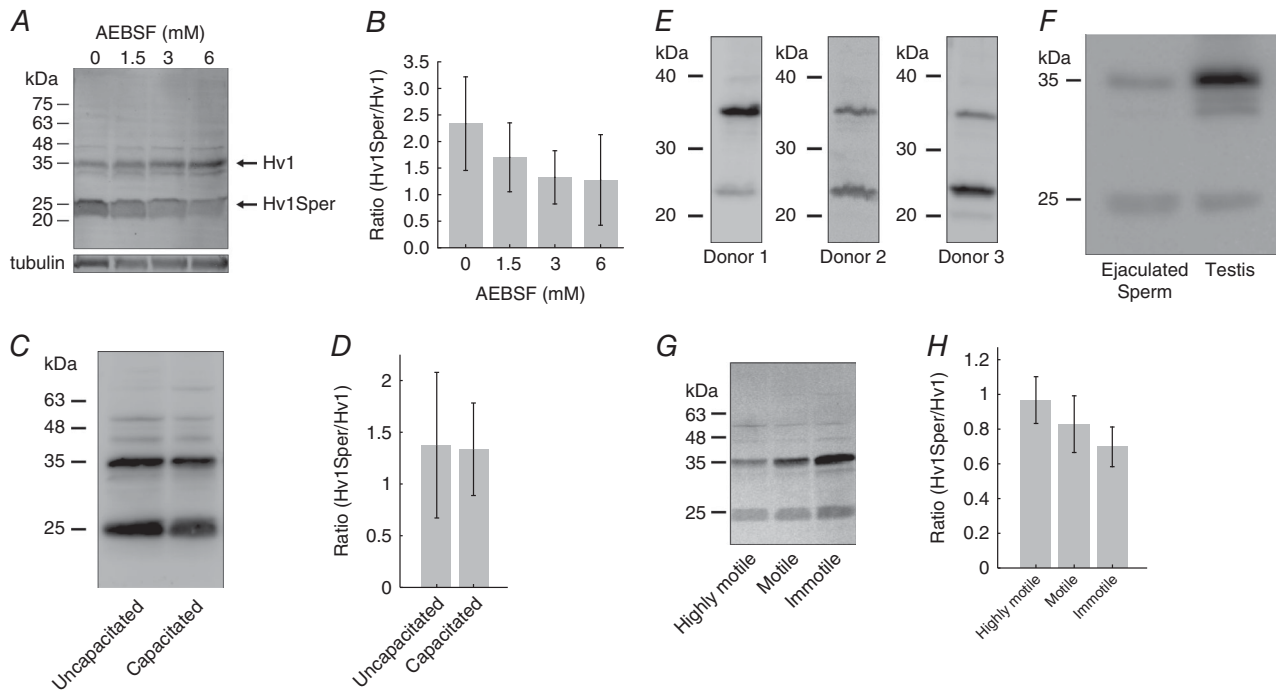


**Figure 3. The Hv1Sper/Hv1 ratio varies among donors and sperm subpopulations, but is independent of capacitation**

A, western blot of sperm lysed in the presence of various AEB SF concentrations, probed with a C-terminal anti-Hv1 antibody. B, mean Hv1Sper/Hv1 ratio at various AEB SF concentrations. C, western blot of uncapacitated and capacitated sperm, probed with a C-terminal anti-Hv1 antibody. D, mean Hv1Sper/Hv1 ratio of uncapacitated and capacitated sperm (uncapacitated,  $1.4 \pm 0.7$ ,  $n = 4$ ; capacitated,  $1.3 \pm 0.5$ ,  $n = 4$ ). E, western blot of sperm from different donors, probed with a C-terminal anti-Hv1 antibody. F, western blot of sperm and testis lysate, probed with a C-terminal anti-Hv1 antibody. G, western blot of highly motile, motile, and immotile sperm subpopulations, probed with a C-terminal anti-Hv1 antibody. H, mean Hv1/Hv1Sper ratio of the three sperm subpopulations (highly motile,  $0.94 \pm 0.13$ ; motile,  $0.81 \pm 0.14$ ; immotile,  $0.67 \pm 0.11$ ;  $n = 4$ ). Error bars indicate the SD.

Sigma-Aldrich (St Louis, MO, USA) or Thermo Fisher Scientific Inc.

## Results

### Human sperm contain full-length Hv1 and a shorter Hv1 variant

Human sperm express the voltage-gated proton channel Hv1 (Lishko *et al.* 2010). To study Hv1 in sperm, we raised a polyclonal antibody directed against the C-terminus of Hv1 (Fig. 1C). The specificity of the anti-Hv1 antibody was tested on heterologously expressed Hv1, tagged at the C-terminus with HA. In western blots of Hv1-HA-transfected HEK293 cells, but not of control cells, an anti-HA and the anti-Hv1 antibody labelled a polypeptide with an apparent molecular weight ( $M_w$ ) of ~35 kDa (Fig. 1A) (Ramsey *et al.* 2006). Omitting the HA-tag lowered the  $M_w$  of the protein detected by the

anti-Hv1 antibody by ~1 kDa (Fig. 1A), consistent with the  $M_w$  of the tag (1.1 kDa). The difference between apparent (34 kDa) and predicted  $M_w$  (31.7 kDa) might be accounted for by an intrinsically disordered region (IDR) (amino acids 54–86) in the N-terminal region of Hv1; IDRs tend to increase the apparent  $M_w$  of proteins (Batra-Safferling *et al.* 2006). In human sperm, the anti-Hv1 antibody detected two bands of approximately 35 and 25 kDa (Fig. 1B), suggesting that sperm harbour Hv1 and a shorter Hv1 variant. To scrutinize this result, we performed protein mass spectrometry. Proteotypic peptides of Hv1 were present in both bands. In the 25 kDa band, we identified a peptide of the N-terminus (amino acids 69–83) and another of the C-terminus (amino acids 265–273) (Fig. 1C), confirming that the 25 kDa band represents a short Hv1 variant. We named this short variant Hv1Sper. In a human monocyte cell line and in human lung epithelium, the anti-Hv1 antibody detected full-length Hv1, but not Hv1Sper, suggesting that this

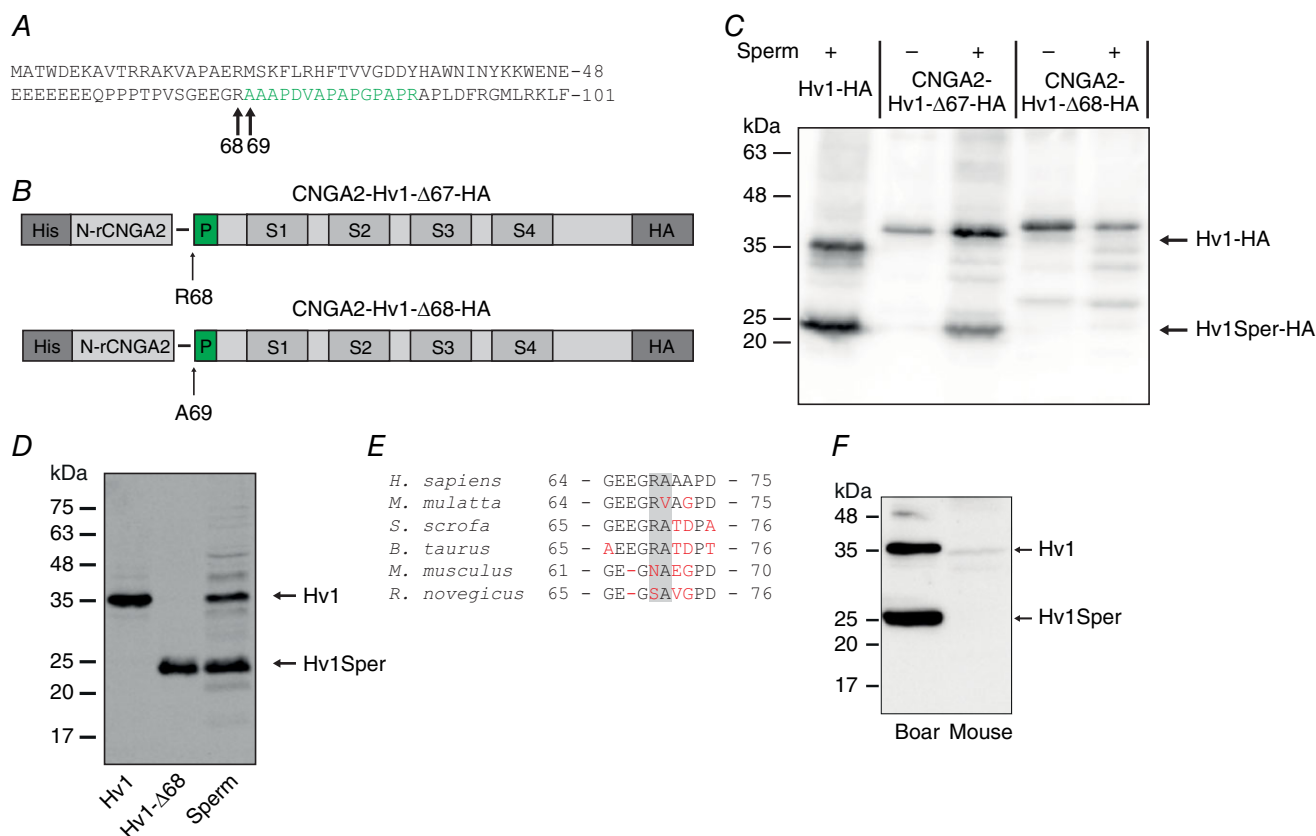


**Figure 4. Hv1 is N-terminally cleaved at position R68**

A, amino acid sequence of the N-terminal part of Hv1. The peptide shown in green was identified by MS in the protein band corresponding to Hv1Sper (Fig. 1B). B, Hv1-HA constructs in which the first 67 (Hv1-Δ67) or 68 amino acids (Hv1-Δ68) were replaced by an N-terminal segment of a CNGA2 channel (His-N-rCNGA2). C, western blot of HEK cells, alone (–) or mixed with sperm (+), expressing Hv1-HA or the CNGA2-Hv1-HA construct, probed with the anti-HA antibody. D, western blot of oocytes expressing Hv1 or Hv1-Δ68 and of human sperm, probed with the C-terminal anti-Hv1 antibody. E, sequence alignment of the N-terminal cleavage site (highlighted in grey) among six mammalian species (human, macaque, boar, bull, mouse, rat; non-conserved amino acids in red). F, western blot of boar and mouse sperm, probed with the C-terminal anti-Hv1 antibody.

short Hv1 form is not commonly expressed and might be specific for sperm (Fig. 1D).

### Hv1 is post-translationally cleaved by a serine protease

Hv1Sper might result from alternative splicing. In the NCBI database, one splice variant of human Hv1 is reported that gives rise to a shorter channel (accession number NP\_001243342) (Hondares *et al.* 2014). This variant lacks the first 20 amino acid residues (calculated  $M_w$  of 29.4 kDa). Hv1Sper is noticeably shorter and lacks  $\geq 60$  amino acid residues. Therefore, we tested whether in sperm, Hv1Sper results from post-translational

proteolytic cleavage of Hv1. We tested this possibility, surmising that the sperm proteases cleave not only native Hv1, but also heterologously expressed Hv1. To this end, lysates of HEK293 cells expressing full-length Hv1-HA were incubated with human sperm lysate (Fig. 2A). In the sperm/HEK cell mix, the anti-HA antibody detected the 35-kDa band but also an additional 26-kDa band, corresponding to cleaved Hv1-HA (i.e. Hv1Sper-HA). With an increasing sperm/HEK cell ratio, the Hv1Sper-HA/Hv1-HA intensity ratio increased from 0.02 up to  $\sim 0.3$  (Fig. 2B). Furthermore, high concentrations of the mammalian protease-inhibitor cocktail mPIC and the specific serine-protease inhibitor AEBSPF prevented the generation of Hv1Sper-HA

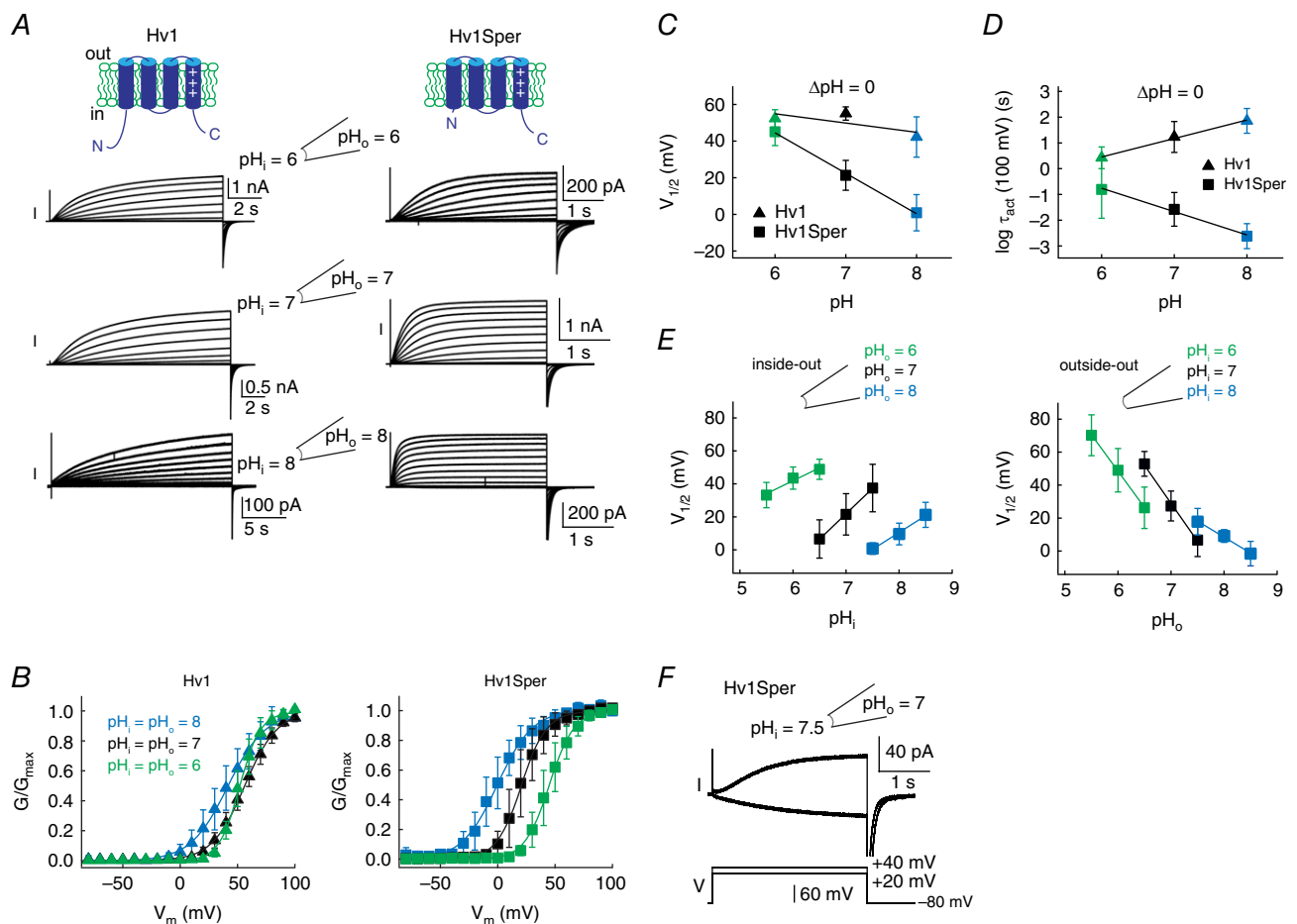


#### Figure 5. Hv1Sper has altered pH-voltage dependence and activation kinetics

A, inside-out patch clamp recording from *X. laevis* oocytes expressing Hv1 (left) or Hv1Sper (right) at  $pH_i = pH_o = 6$  (top), 7 (middle) and 8 (bottom). Voltage steps of increasing amplitudes ( $-80$  to  $+100$  mV in 10 mV increments) elicited voltage-dependent outward currents. B, GV relationships derived from tail currents at the three different pH conditions (leaving  $\Delta pH = 0$ ), fitted with a single Boltzmann function. C, half-maximal activation voltage ( $V_{1/2}$ ) derived from the Boltzmann fits of the data in (B). D, activation-time constants of Hv1Sper and Hv1 obtained from single (Hv1Sper) and weighted double (Hv1) exponential fits. E, voltage of half-maximal activation ( $V_{1/2}$ ) as a function of changes in  $pH_i$  and  $pH_o$  in the inside-out (left) and outside-out (right) configuration. The shift of  $V_{1/2}$  in the inside-out configuration for  $pH_o$  of 6, 7 and 8 was  $-15.6$ ,  $-30.9$  and  $-20.4$  mV/pH unit, respectively. The shift of  $V_{1/2}$  in the outside-out configuration for  $pH_i$  of 6, 7 and 8 was  $-44$ ,  $-46$  and  $-19.4$  mV/pH unit, respectively. F, inward and outward currents of Hv1Sper, depending on the pH conditions. Error bars indicate the SD.

(Fig. 2C), whereas the cysteine-protease inhibitor E64 had no effect. We conclude that Hv1Sper results from post-translational cleavage of Hv1 by a serine protease.

Hv1Sper might be generated during lysis of sperm. To confirm that Hv1Sper exists in intact sperm, we prepared lysates of sperm in the absence and presence of increasing AEBSF concentrations. The Hv1Sper/Hv1 ratio slightly decreased with increasing AEBSF concentrations (Fig. 3A and B), indicating that only a small fraction of Hv1 is cleaved upon sperm lysis. For AEBSF  $\geq 3$  mM, the Hv1Sper/Hv1 ratio became constant, reflecting the relative abundance of the two isoforms in intact sperm. Of note, the Hv1Sper/Hv1 ratio varied considerably among donors (Fig. 3E).

During capacitation, a maturation process of sperm, proton currents in human sperm are enhanced (Lishko *et al.* 2010) by an unknown mechanism. We tested whether this mechanism involves production of Hv1Sper. However, the Hv1Sper/Hv1 ratio was similar in uncapacitated and capacitated sperm (Fig. 3C and D). Furthermore, we identified Hv1Sper also in human testis lysates (Fig. 3F), indicating that Hv1Sper is produced

during spermatogenesis. When populations of ejaculated sperm were separated by density gradient centrifugation, Hv1Sper was enriched in highly motile sperm compared to motile and immotile sperm (Fig. 3G and H), suggesting that Hv1Sper might be required for sperm motility.

### Hv1 is N-terminally cleaved between position R68 and A69

Hv1Sper might result from proteolytic cleavage of Hv1 in the C- or N-terminal region, which are both located intracellularly. However, two independent findings exclude a C-terminal cleavage: MS analysis of the 25 kDa Hv1Sper band identified a tryptic peptide of the very C-terminus, (Fig. 1C) and the antibody that recognizes both Hv1 and Hv1Sper is directed against the C-terminus. Therefore, we suspected that Hv1 is cleaved at the N-terminal IDR that ranges from amino acid E54 to L86. IDRs lack secondary structure and expose proteolytic cleavage sites (Linding *et al.* 2003; Dyson and Wright 2005). MS analysis of Hv1Sper identified the N-terminal peptide A69-R83

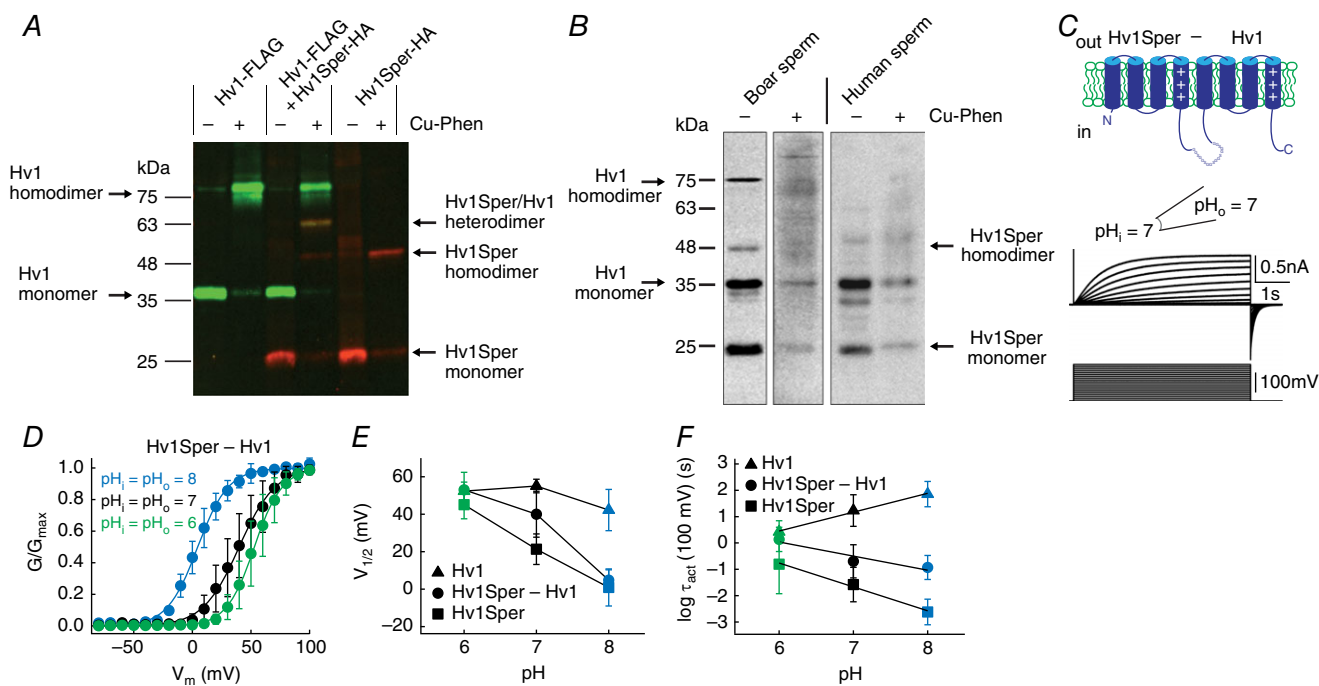


**Figure 6. Hv1Sper and Hv1 form heterodimers with unique biophysical properties**

A, western blot of *X. laevis* oocytes expressing Hv1-FLAG or Hv1Sper-HA, or both, in the presence or absence of the oxidant Cu-phenanthroline, probed with an anti-FLAG (green) and anti-HA (red) antibody. B, western blot of boar and human sperm incubated in the presence or absence of the cysteine cross-linker Cu-phenanthroline (Cu-Phen), probed with a C-terminal anti-Hv1 antibody. C, inside-out patch clamp recording from *Xenopus* oocytes expressing a tandem heterodimer consisting of Hv1Sper linked to Hv1 with a flexible linker, recorded at  $pH_i = pH_o = 7$ . Voltage steps of increasing amplitudes ( $-80$  to  $+100$  mV) elicited voltage-dependent outward currents. D, GV relationships derived from tail currents at three different pH conditions (leaving  $\Delta pH = 0$ ), fitted with a single Boltzmann function. E, half-maximal activation voltage ( $V_{1/2}$ ) derived from the Boltzmann fits shown in (C) (Hv1 and Hv1Sper taken from Fig. 5C). F, activation time constants of the Hv1Sper-Hv1 tandem heterodimer, as well as Hv1 and Hv1Sper (taken from Fig. 5D). Error bars indicate the SD.



(Fig. 4A), indicating that Hv1 is cleaved within the IDR upstream of A69. Trypsin-like serine proteases cleave peptide bonds following a positively-charged amino acid. Indeed, one potential cleavage site is between R68 and A69; cleavage at this site would result in a protein with an expected  $M_w$  of 23.7 kDa, compatible with the apparent  $M_w$  (25 kDa) of Hv1Sper.

To identify the cleavage site, we replaced the N-terminus of Hv1-HA before or after the presumed cleavage site R68-A69 by the N-terminus of a cyclic nucleotide-gated (CNGA2) channel (Fig. 4B) and incubated the CNGA2-Hv1-HA fusion constructs with sperm lysate; the CNGA2 domain served to enhance the  $M_w$  of the constructs, ensuring a readily detectable mass shift upon their cleavage. Constructs that contained R68-A69 (CNGA2-Hv1- $\Delta$ 67-HA) yielded Hv1Sper-HA, as indicated by a 25 kDa band, whereas constructs that lacked R68-A69 (CNGA2-Hv1- $\Delta$ 68-HA) did not yield Hv1Sper-HA (Fig. 4C). Moreover, the  $M_w$  of heterologously expressed Hv1- $\Delta$ 68 and native Hv1Sper were identical (Fig. 4D). Altogether, we conclude that A69 is the first amino acid residue of Hv1Sper. The R68 cleavage site and the expression of Hv1 and Hv1Sper in sperm is conserved in some but not all mammalian species (Fig. 4E): boar sperm harbour both Hv1 and Hv1Sper (Fig. 4F), whereas mouse sperm do not express the channel at all (Fig. 4F) (Lishko *et al.* 2010). Mouse Hv1 lacks the cleavage site (position 68 is an asparagine) (Fig. 4E). Therefore, it would be interesting to study whether the expression of Hv1 in sperm correlates with the conservation of R68 in other species.

### The pH control of Hv1Sper is altered

We studied the electrophysiological properties of Hv1Sper (Hv1- $\Delta$ 68) and Hv1 by heterologous expression in *X. laevis* frog oocytes. Currents were recorded from excised patches in the voltage clamp mode. At an intra- and extracellular pH of 6 ( $\Delta$ pH = 0), activation kinetics and voltage of half-maximal activation ( $V_{1/2}$ ) of Hv1 and Hv1Sper were rather similar (Fig. 5A–D and Table 1). However, an increase of  $pH_i$  and  $pH_o$  leaving  $\Delta$ pH = 0, shifted the  $V_{1/2}$  of Hv1Sper by  $-22$  mV/pH unit (Fig. 5B and C), whereas the  $V_{1/2}$  of Hv1 was shifted only by  $-5$  mV/pH unit. Moreover, the pH increase strongly accelerated the activation kinetics of Hv1Sper, whereas activation of Hv1 was decelerated ( $\Delta \log(\tau_{act})/pH$  unit =  $-0.9$  vs.  $+0.7$ ; at  $+100$  mV) (Fig. 5A and D). However, the pH dependence of the slopes of the GV<sub>s</sub> was similar in Hv1 and Hv1Sper (Table 1). Thus, the N-terminal cleavage renders Hv1Sper sensitive to the pH itself on both sides of the membrane. We tested whether the sensitivity of Hv1Sper to pH itself compromised the sensitivity to pH changes on either side of the membrane

(i.e.  $\Delta$ pH sensing) (Fig. 5E). Similar to Hv1 (Cherny *et al.* 2015),  $\Delta$ pH sensing in Hv1Sper appears to saturate at alkaline pH: at both extracellular and intracellular pH 8, the  $V_{1/2}$  shifted only by  $\sim 20$  mV/pH unit (Fig. 5E). At an intracellular pH of 6 and 7, changes in  $pH_o$  shifted the  $V_{1/2}$  of Hv1Sper by  $\sim 45$  mV/pH unit. However, at an extracellular pH of 6 and 7, changes in  $pH_i$  shifted the  $V_{1/2}$  by only 15 and 30 mV/pH unit, respectively (Fig. 5E). This indicates that, in Hv1Sper, the sensing of changes in  $pH_i$ , but not that of  $pH_o$ , is compromised. Altogether, we conclude that the N-terminus is involved but not required for  $\Delta$ pH sensing in Hv1. Instead, the presence or absence of the N-terminus determines whether the channel senses  $\Delta$ pH only or both  $\Delta$ pH and pH itself. Notably, as a result of the dual control by both pH and  $\Delta$ pH, Hv1Sper conducts inward proton currents within a small, yet physiologically significant range of  $V_m$  and pH values (Fig. 5F). Thus, Hv1 can exclusively export protons and thereby alkalize sperm, whereas Hv1Sper might either alkalize or acidify sperm, depending on the electrochemical conditions.

### Hv1Sper and Hv1 form heterodimers

Hv1 assembles as a dimer via a coiled-coil domain in the C-terminus (Lee *et al.* 2008). By chemical cross-linking, we studied whether Hv1Sper forms homodimers and/or heterodimers with Hv1. Hv1 and Hv1Sper carry a cysteine at position C249 that allows for cross-linking using copper phenanthroline as oxidant (Lee *et al.* 2008). FLAG-tagged Hv1 and HA-tagged Hv1Sper were expressed in *Xenopus* oocytes. Cross-link products were analysed by western blotting, using anti-FLAG and anti-HA antibodies. If Hv1Sper forms both homodimers and heterodimers with Hv1, three different dimeric cross-link species are expected: Hv1 homodimers, Hv1Sper homodimers, and Hv1/Hv1Sper heterodimers. Altogether, we expect five molecular species with an apparent  $M_w$  of  $\sim 26$  kDa (Hv1Sper monomer), 36 kDa (Hv1 monomer), 52 kDa (Hv1Sper homodimer), 62 kDa (Hv1Sper/Hv1 heterodimer), and 72 kDa (Hv1 homodimer). Hv1 and Hv1Sper monomers and homodimers are detected exclusively by the anti-FLAG and anti-HA antibody, respectively, whereas both antibodies detect Hv1Sper/Hv1 heterodimers. Indeed, these predictions were borne out by cross-linking experiments: five molecular species with an apparent  $M_w$  of 25.5 kDa, 37 kDa, 51 kDa, 63 kDa, and 75 kDa were identified (Fig. 6A); the 63 kDa band was detected by both antibodies. In conclusion, Hv1 and Hv1Sper form homodimers and, when co-expressed, Hv1 and Hv1Sper form heterodimers.

We examined whether Hv1Sper/Hv1 heterodimers also exist in human and boar sperm. In boar sperm, even in the absence of the cross-linker and under non-reducing conditions, the antibody recognized both monomeric and

**Table 1. Fit parameters for the GV relationships of different Hv1 constructs (mean  $\pm$  SD)**

Channel	pH <sub>i</sub> /pH <sub>o</sub>	V <sub>1/2</sub> (mV)	kT/ze <sub>o</sub> (mV)	n
Hv1	6/6	52.4 $\pm$ 4.8	9 $\pm$ 2	4
	7/7	55.1 $\pm$ 3.6	14.4 $\pm$ 0.9	6
	8/8	42.2 $\pm$ 11	15.5 $\pm$ 1.6	7
Hv1Sper (Hv1- $\Delta$ 68)	6/6	45.1 $\pm$ 7.5	10 $\pm$ 1.2	3
	7/7	21.4 $\pm$ 8.2	10 $\pm$ 2.4	11
	8/8	0.9 $\pm$ 9.9	13.8 $\pm$ 1.9	10
Hv1Sper-Hv1	6/6	53.1 $\pm$ 9.3	10.8 $\pm$ 1.7	4
	7/7	40 $\pm$ 12.2	13.9 $\pm$ 1.3	4
	8/8	4.8 $\pm$ 5.5	12.7 $\pm$ 2.2	4
Hv1 + Hv1Sper	6/6	49.3 $\pm$ 4.6	10.8 $\pm$ 0.9	7
	7/7	30.8 $\pm$ 3	14.5 $\pm$ 3.1	7
	8/8	18.6 $\pm$ 12.8	16.8 $\pm$ 2.3	4

homodimeric Hv1 and Hv1Sper but no Hv1Sper/Hv1 heterodimer ( $M_w \approx 60$  kDa). Upon cross-linking, the monomer and homodimer bands diminished and a smear of bands evolved at  $>35$  kDa (Fig. 6B). In human sperm, in the absence of the cross-linker, the antibody recognized monomeric Hv1 and Hv1Sper but no bands corresponding to the homodimers (Fig. 6B); instead, two faint bands at  $\sim 50$  and 60 kDa were recognized. At any concentration and incubation time, cross-linking diminished Hv1 and Hv1Sper monomers and produced a smear of bands at  $>35$  kDa. Altogether, whether Hv1Sper and Hv1 form heterodimers in sperm is unclear.

### Hv1Sper-Hv1 tandem dimers display distinct pH- and voltage dependence

In the Hv1 dimer, subunits gate co-operatively (Gonzalez *et al.* 2010; Tombola *et al.* 2010). Thus, we tested whether gating of Hv1Sper/Hv1 heterodimers differs from that of homodimers. To confirm a 1:1 ratio of Hv1Sper and Hv1 and to enforce heteromerization, we constructed an Hv1Sper-Hv1 tandem heterodimer; the channels were connected with a flexible 18 amino acid linker (Fig. 6C). A similar construct assembled as a pseudo-dimer (Tombola *et al.* 2008). The pH dependence of the Hv1Sper-Hv1 tandem was distinct from that of Hv1 and Hv1Sper homodimers (Fig. 6D-F and Table 1): at pH<sub>i</sub> = pH<sub>o</sub> = 6, the activation kinetics and V<sub>1/2</sub> of Hv1Sper-Hv1, Hv1, and Hv1Sper were similar. At pH<sub>i</sub> = pH<sub>o</sub> = 7, the V<sub>1/2</sub> of Hv1Sper-Hv1 was shifted to more negative potentials and became intermediate between that of Hv1 and Hv1Sper. At pH<sub>i</sub> = pH<sub>o</sub> = 8, however, the V<sub>1/2</sub> of Hv1Sper-Hv1 and Hv1Sper became similar again (Fig. 6D and E and Table 1). The activation kinetics of Hv1Sper-Hv1 was intermediate between that of Hv1 and Hv1Sper at all tested pH values (Fig. 6F). Thus, even in a heterodimer, in which one subunit lacks the N-terminus, gating is controlled

both by  $\Delta$ pH and pH itself. However, the pH sensitivity is attenuated and kicks in at a more alkaline pH than in Hv1Sper homodimers. This finding highlights the interplay of subunits during gating and demonstrates that in a heterodimer, gating characteristics can be dominated by one of the subunits. Of note, co-expression of Hv1 and Hv1Sper at a 1:1 ratio yielded results similar to those of the tandem dimer (Table 1).

Finally, we studied proton currents in human sperm. At pH<sub>i</sub> = pH<sub>o</sub> = 6, we recorded sizeable proton currents. Outward currents commenced at V<sub>m</sub> = +30 mV (Fig. 7A),  $\sim 20$  mV more positive than currents carried by heterologous Hv1, Hv1Sper, and Hv1Sper-Hv1 (Figs 5B and 6D). This difference of activation thresholds between native and heterologous Hv1 currents is a well-known, yet unexplained phenomenon (Musset *et al.* 2008). At pH<sub>i</sub> = pH<sub>o</sub> = 7, current amplitudes were only 20% of those at pH<sub>i</sub> = pH<sub>o</sub> = 6, and, at pH  $> 7$ , currents were completely abolished (Fig. 7A, B). This is probably a result of the low numbers of protons available in the small intracellular volume (i.e. flagellum  $\approx 2.5$  fl; head  $\approx 62.5$  fl). The large decrease of current amplitudes at pH  $> 6$  paired with the more positive activation threshold of native Hv1 currents prevented us from determining the relative contribution of Hv1, Hv1Sper, and potential Hv1Sper-Hv1 heteromers to proton currents in sperm. We considered whether the contribution of Hv1 and Hv1Sper might instead be identified by pharmacology. However, both Zn<sup>2+</sup> and 2GBI (Ramsey *et al.* 2006; Hong *et al.* 2013), two Hv1 inhibitors, also inhibit Hv1Sper (Fig. 7B). Thus, the available pharmacological tools are ill-suited for revealing the composition of proton currents in human sperm.

## Discussion

In the present study, we show that human sperm harbour a Hv1 variant, Hv1Sper, that lacks the first 68 amino acids of

the N-terminus as a result of proteolytic cleavage. Gating of Hv1 by voltage is intimately coupled to  $\Delta\text{pH}$  across the cell membrane. In Hv1Sper, the voltage-dependence of gating is modulated not only by  $\Delta\text{pH}$ , but also by changes in  $\text{pH}_i$  and  $\text{pH}_o$  that keep  $\Delta\text{pH}$  constant. This indicates that the first 68 amino acids of the N-terminus are not required for  $\Delta\text{pH}$  sensing but render Hv1 insensitive to the pH itself. This ensures that Hv1 carries only proton outward currents that alkalize the cell.

The  $V_{1/2}$  of Hv1 shifts to more positive and negative potentials at  $\text{pH}_i > \text{pH}_o$  and  $\text{pH}_i < \text{pH}_o$ , respectively. The insensitivity of Hv1 to a simultaneous change of  $\text{pH}_i$  and  $\text{pH}_o$  that leave  $\Delta\text{pH}$  constant (referred to as change in pH itself) demonstrates that  $\Delta\text{pH}$  sensing involves more than a simple protonation/deprotonation of titratable residues. Hv1Sper lacks 68 amino acids of the N-terminus, which face the intracellular side. The attenuated sensitivity of Hv1Sper to  $\text{pH}_i$  changes (Fig. 5E) suggests that these amino acids are involved in  $\text{pH}_i$  sensing; the imbalanced  $\text{pH}_i$  vs.  $\text{pH}_o$  sensing might underlie the control of Hv1Sper by pH itself. It also suggests that there are distinct intra- and extracellular pH sensors. Nevertheless, the exact mechanisms and residues conveying  $\Delta\text{pH}$  sensitivity still remain elusive. Even an exhaustive mutagenesis study only identified mutants that diminish or enhance but do not abolish  $\Delta\text{pH}$  sensing (Ramsey *et al.* 2010). It was proposed that the local proton concentration is coupled to the movement of the voltage sensor by electrostatic interaction of protonated water molecules in the central VSD crevice with voltage-sensing arginine residues in S4 (Ramsey *et al.* 2010). However, cleavage of the entire N-terminus (amino acids 1–96, hHv1- $\Delta\text{N}$ ) evoked the most pronounced decrease in  $\Delta V_{1/2}/\Delta\text{pH}$  unit. Altogether, these findings suggest that both  $\Delta\text{pH}$  and pH sensing is modulated by the N-terminus.

The N-terminus of Hv1 contains an IDR, indicating that part of the N-terminus is flexible. The N-terminus might interact in a pH-dependent manner with intracellular sites of the VSD and, thereby, determine the pH-control of gating. For example, Hv1Sper lacks a cluster of eight glutamates (amino acids 48–55) that in Hv1, might electrostatically interact with positively-charged, intracellular residues of S1, S4, and the S2–S3 loop. This interaction could affect the binding of protons to the S4 voltage sensor, rendering full-length Hv1 largely insensitive to changes in pH itself. Recently, we showed that S1 undergoes conformational changes concomitant with channel opening (Mony *et al.* 2015). This suggests that S1 forms part of the gate and the N-terminus could restrict conformational changes of S1, altering channel gating. Supporting this notion, phosphorylation of T29 by protein kinase C (PKC) shifts the  $V_{1/2}$  of Hv1 to more negative potentials, increases the maximal conductance and accelerates activation kinetics (Musset *et al.* 2008). The Hv1 splice variant that lacks the first 20 amino acids is more strongly affected by T29 phosphorylation (Hondares *et al.* 2014). Whether the gating of this isoform is also modulated by the pH itself is unknown.

Transient interactions between the N-terminus and transmembrane segments are common in other ion channels. In classical voltage-gated cation channels, a rapid inactivation mediated by the N-terminus blocks the channel in the open state ('ball-and-chain' mechanism) (Armstrong and Bezanilla, 1977). In the voltage-sensing phosphatase, consisting of a VSD linked to an enzymatic phosphatase domain, the N-terminus undergoes pronounced voltage-dependent conformational changes that can be detected by Förster resonance energy transfer (Tsutsui *et al.* 2013). A similar Förster resonance

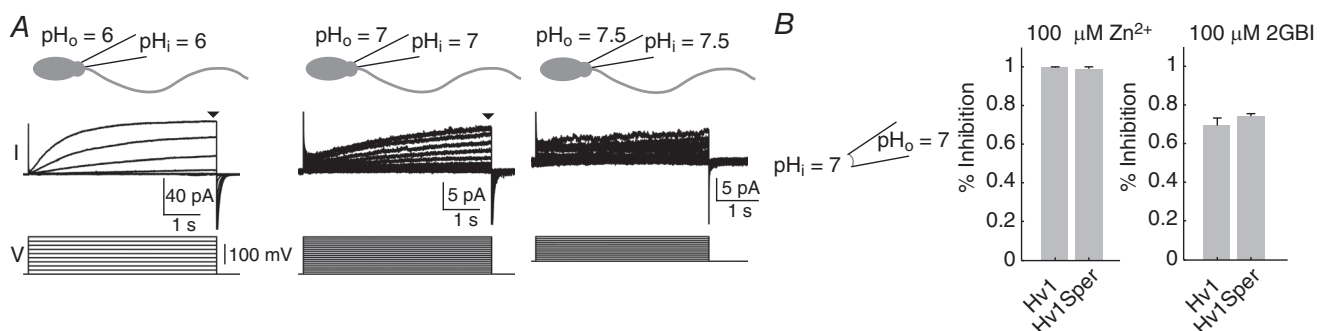


**Figure 7. Control of sperm proton currents by pH and block of Hv1Sper by  $\text{Zn}^{2+}$  and 2GBI**

A, whole-cell patch clamp recording from human sperm at  $\text{pH}_i = \text{pH}_o = 6, 7$ , and 7.5. Voltage-dependent outward currents (top traces) evoked by voltage steps (bottom traces) of increasing amplitude ( $-80$  to  $+100$  mV, pH 6 and 7;  $-20$  to  $+100$  mV, pH 7.5). B, inhibition of outward currents in excised patches of *X. laevis* oocytes heterologously expressing Hv1 or Hv1Sper by extracellular  $\text{Zn}^{2+}$  and intracellular 2GBI at  $\text{pH}_i = \text{pH}_o = 7$ . Currents were evoked by a voltage step from  $-80$  mV to  $+80$  mV ( $\text{Zn}^{2+}$ : Hv1  $99.7 \pm 0.3\%$  inhibition,  $n = 3$ ; Hv1Sper  $98.9 \pm 1\%$ ,  $n = 4$ ; 2GBI: Hv1  $69.4 \pm 3.7\%$  inhibition,  $n = 3$ ; Hv1Sper  $74.2 \pm 1.4\%$ ,  $n = 3$ ). Error bars indicate the SD.

energy transfer-based approach might be suited to study whether the N-terminus in Hv1 does indeed interact with the VSD in a pH-dependent manner.

In sperm, Hv1 has been proposed to serve as a key regulator of  $\text{pH}_i$  and, thereby, sperm function and fertilization. In the oviduct, sperm undergo a maturation process, called capacitation (Austin, 1951; Chang, 1951; Visconti *et al.* 1995a; Visconti *et al.* 1995b). The complex physiological mechanisms underlying capacitation are not well understood. Among other cellular events, the cytosol alkalinizes and intracellular  $\text{Ca}^{2+}$  levels increase, which changes the flagellar beat. In capacitated sperm, proton currents are enhanced and 1 mM  $\text{Zn}^{2+}$  suppresses sperm capacitation, suggesting that Hv1 is involved in capacitation (Lishko *et al.* 2010). Hv1 has also been implicated in sperm superoxide production (Musset *et al.* 2012). During their journey across the male and female genital tract, sperm experience an ever-increasing  $\text{pH}_o$ , ranging from around pH 6 in the epididymis up to pH 8.2 in the distal oviduct. A  $\Delta\text{pH}$ -evoked proton efflux via Hv1 has been proposed to couple  $\text{pH}_o$  to changes in  $\text{pH}_i$  and thereby intracellular  $\text{Ca}^{2+}$  levels. As a result of the control by the pH itself, Hv1Sper might ensure a more sustained proton efflux from sperm over a certain range of  $\text{pH}_o$  in the oviduct. However, under alkaline conditions, Hv1Sper activates negative to the Nernst potential for protons and might mediate a proton influx that acidifies the cell. Moreover, heterologously expressed Hv1 is gated by mechanical stimuli (Pathak *et al.* 2016). This suggests that in sperm, the channel can be activated by hydrodynamic shear forces or collisions with the epithelium that lines the female genital tract. Functional studies are required to establish or refute the hypothesis that Hv1 and Hv1Sper control sperm function and also to unravel the specific role of Hv1Sper. Indeed, Hv1 and Hv1Sper might be involved in testicular spermatogenesis or epididymal sperm maturation rather than in the  $\text{pH}_i$  control of mature sperm.

Cleavage of Hv1 is conserved in human and boar sperm. In mouse sperm, Hv1 is absent altogether (Lishko *et al.* 2010) and the R68 cleavage site is not conserved in mouse Hv1 (position 68 is an asparagine). It would be interesting to determine whether Hv1 expression in mammalian sperm is tied to the conservation of the cleavage site. Post-translational cleavage has been reported for several other channels in sperm flagella and also cilia. Cleaved isoforms of the  $\text{Ca}^{2+}$  channels CatSper and the  $\text{K}^+$  channel Slo3 were identified in mouse and human sperm, respectively (Brenker *et al.* 2014; Chung *et al.* 2014). Moreover, sea urchin sperm harbour a cleaved  $\text{K}^+$ -selective CNG channel (Bönigk *et al.* 2009) and, finally, the CNG channel of rod photoreceptors is post-translationally cleaved (Molday *et al.* 1991). The physiological consequences of channel cleavages are unknown.

## References

- Armstrong CM & Bezanilla F (1977). Inactivation of the sodium channel. II. Gating current experiments. *J Gen Physiol* **70**, 567–590.
- Austin CR (1951). Observations on the penetration of the sperm in the mammalian egg. *Aust J Sci Res B* **4**, 581–596.
- Batra-Safferling R, Abarca-Heidemann K, Körschen HG, Tziatzios C, Stoldt M, Budyak I, Willbold D, Schwalbe H, Klein-Seetharaman J & Kaupp UB (2006). Glutamic acid-rich proteins of rod photoreceptors are natively unfolded. *J Biol Chem* **281**, 1449–1460.
- Berger TK & Isacoff EY (2011). The pore of the voltage-gated proton channel. *Neuron* **72**, 991–1000.
- Bönigk W, Loogen A, Seifert R, Kashikar N, Klemm C, Krause E, Hagen V, Kremmer E, Strünker T & Kaupp UB (2009). An atypical CNG channel activated by a single cGMP molecule controls sperm chemotaxis. *Sci Signal* **2**, ra68.
- Brenker C, Goodwin N, Weyand I, Kashikar ND, Naruse M, Krähling M, Müller A, Kaupp UB & Strünker T (2012). The CatSper channel: a polymodal chemosensor in human sperm. *EMBO J* **31**, 1654–1665.
- Brenker C, Zhou Y, Müller A, Echeverry FA, Trötschel C, Poetsch A, Xia X-M, Bönigk W, Lingle CJ, Kaupp UB & Strünker T (2014). The  $\text{Ca}^{2+}$ -activated  $\text{K}^+$  current of human sperm is mediated by Slo3. *Elife* **3**, e01438.
- Capasso M, Bhamrah MK, Henley T, Boyd RS, Langlais C, Cain K, Dinsdale D, Pulford K, Khan M, Musset B, Cherny VV, Morgan D, Gascoyne RD, Vigorito E, DeCoursey TE, MacLennan ICM & Dyer MJS (2010). HVCN1 modulates BCR signal strength via regulation of BCR-dependent generation of reactive oxygen species. *Nat Immunol* **11**, 265–272.
- Chang MC (1951). Fertilizing capacity of spermatozoa deposited into the fallopian tubes. *Nature* **168**, 697–698.
- Cherny VV, Markin VS & DeCoursey TE (1995). The voltage-activated hydrogen ion conductance in rat alveolar epithelial cells is determined by the pH gradient. *J Gen Physiol* **105**, 861–896.
- Cherny VV, Morgan D, Musset B, Chaves G, Smith SM & DeCoursey TE (2015). Tryptophan 207 is crucial to the unique properties of the human voltage-gated proton channel, hHv1. *J Gen Physiol* **146**, 343–356.
- Chung J-J, Shim S-H, Everley RA, Gygi SP, Zhuang X & Clapham DE (2014). Structurally distinct  $\text{Ca}^{2+}$  signalling domains of sperm flagella orchestrate tyrosine phosphorylation and motility. *Cell* **157**, 808–822.
- Dyson HJ & Wright PE (2005). Intrinsically unstructured proteins and their functions. *Nat Rev Mol Cell Biol* **6**, 197–208.
- El Chemaly A, Okochi Y, Sasaki M, Arnaudeau S, Okamura Y & Demaurex N (2010). VSOP/Hv1 proton channels sustain calcium entry, neutrophil migration, and superoxide production by limiting cell depolarization and acidification. *J Exp Med* **207**, 129–139.
- Gonzalez C, Koch HP, Drum BM & Larsson HP (2010). Strong cooperativity between subunits in voltage-gated proton channels. *Nat Struct Mol Biol* **17**, 51–56.



- Henderson LM, Chappell JB & Jones OT (1987). The superoxide-generating NADPH oxidase of human neutrophils is electrogenic and associated with an H<sup>+</sup> channel. *Biochem J* **246**, 325–329.
- Hondares E, Brown MA, Musset B, Morgan D, Cherny VV, Taubert C, Bhamrah MK, Coe D, Marelli-Berg F, Gribben JG, Dyer MJS, DeCoursey TE & Capasso M (2014). Enhanced activation of an amino-terminally truncated isoform of the voltage-gated proton channel HVCN1 enriched in malignant B cells. *Proc Natl Acad Sci USA* **111**, 18078–18083.
- Hong L, Pathak MM, Kim IH, Ta D & Tombola F (2013). Voltage-sensing domain of voltage-gated proton channel hv1 shares mechanism of block with pore domains. *Neuron* **77**, 274–287.
- Iovannisci D, Illek B & Fischer H (2010). Function of the HVCN1 proton channel in airway epithelia and a naturally occurring mutation, M91T. *J Gen Physiol* **136**, 35–46.
- Koch HP, Kurokawa T, Okochi Y, Sasaki M, Okamura Y & Larsson HP (2008). Multimeric nature of voltage-gated proton channels. *Proc Natl Acad Sci USA* **105**, 9111–9116.
- Lee S-Y, Letts JA & MacKinnon R (2008). Dimeric subunit stoichiometry of the human voltage-dependent proton channel Hv1. *Proc Natl Acad Sci USA* **105**, 7692–7695.
- Linding R, Russell RB, Neduva V & Gibson TJ (2003). Globplot: Exploring protein sequences for globularity and disorder. *Nucleic Acids Res*, **31**, 3701–3708.
- Lishko PV, Botchkina IL, Fedorenko A & Kirichok Y (2010). Acid extrusion from human spermatozoa is mediated by flagellar voltage-gated proton channel. *Cell* **140**, 327–337.
- Molday RS, Molday LL, Dosé A, Clark-Lewis I, Illing M, Cook NJ, Eismann E & Kaupp UB (1991). The cGMP-gated channel of the rod photoreceptor cell characterization and orientation of the amino terminus. *J Biol Chem* **266**, 21917–21922.
- Mony L, Berger TK & Isacoff EY (2015). A specialized molecular motion opens the Hv1 voltage-gated proton channel. *Nat Struct Mol Biol* **22**, 283–290.
- Musset B, Cherny VV, Morgan D, Okamura Y, Ramsey IS, Clapham DE & DeCoursey TE (2008). Detailed comparison of expressed and native voltage-gated proton channel currents. *J Physiol* **586**, 2477–2486.
- Musset B, Smith SME, Rajan S, Morgan D, Cherny VV & DeCoursey TE (2011). Aspartate112 is the selectivity filter of the human voltage-gated proton channel. *Nature* **480**, 273–277.
- Musset B, Clark RA, DeCoursey TE, Petheo GL, Geiszt M, Chen Y, Cornell JE, Eddy CA, Brzyski RG & El Jamali A (2012). Nox5 in human spermatozoa: expression, function & regulation. *J Biol Chem* **287**, 9376–9388.
- Pathak MM, Tran T, Hong L, Joós B, Morris CE, Tombola F (2016). The Hv1 proton channel responds to mechanical stimuli. *J Gen Physiol* **148**, 405–418.
- Ramsey IS, Mokrab Y, Carvacho I, Sands ZA, Sansom MSP & Clapham DE (2010). An aqueous H<sup>+</sup> permeation pathway in the voltage-gated proton channel Hv1. *Nat Struct Mol Biol* **17**, 869–875.
- Ramsey IS, Moran MM, Chong JA & Clapham DE (2006). A voltage-gated proton-selective channel lacking the pore domain. *Nature* **440**, 1213–1216.
- Ramsey IS, Ruchti E, Kaczmarek JS & Clapham DE (2009). Hv1 proton channels are required for high-level NADPH oxidase-dependent superoxide production during the phagocyte respiratory burst. *Proc Natl Acad Sci USA* **106**, 7642–7647.
- Sasaki M, Takagi M & Okamura Y (2006). A voltage sensor-domain protein is a voltage-gated proton channel. *Science* **312**, 589–592.
- Strünker T, Goodwin N, Brenker C, Kashikar ND, Weyand I, Seifert R & Kaupp UB (2011). The CatSper channel mediates progesterone-induced Ca<sup>2+</sup> influx in human sperm. *Nature* **471**, 382–386.
- Strünker T, Weyand I, Bönigk W, Van Q, Loogen A, Brown JE, Kashikar N, Hagen V, Krause E & Kaupp UB (2006). A K<sup>+</sup>-selective cGMP-gated ion channel controls chemosensation of sperm. *Nat Cell Biol* **8**, 1149–1154.
- Taylor AR, Chrachri A, Wheeler G, Goddard H & Brownlee C (2011). A voltage-gated H<sup>+</sup> channel underlying pH homeostasis in calcifying coccolithophores. *PLoS Biol* **9**, e1001085.
- Tombola F, Ulbrich MH & Isacoff EY (2008). The voltage-gated proton channel Hv1 has two pores, each controlled by one voltage sensor. *Neuron* **58**, 546–556.
- Tombola F, Ulbrich MH, Kohout SC & Isacoff EY (2010). The opening of the two pores of the Hv1 voltage-gated proton channel is tuned by cooperativity. *Nat Struct Mol Biol* **17**, 44–50.
- Visconti PE, Bailey JL, Moore GD, Pan D, Olds-Clarke P & Kopf GS (1995a). Capacitation of mouse spermatozoa. I. Correlation between the capacitation state and protein tyrosine phosphorylation. *Development* **121**, 1129–1137.
- Visconti PE, Moore GD, Bailey JL, Leclerc P, Connors SA, Pan D, Olds-Clarke P & Kopf GS (1995b). Capacitation of mouse spermatozoa. II. Protein tyrosine phosphorylation and capacitation are regulated by a cAMP-dependent pathway. *Development* **121**, 1139–1150.
- Wang Y, Li SJ, Wu X, Che Y & Li Q (2012). Clinicopathological and biological significance of human voltage-gated proton channel Hv1 protein overexpression in breast cancer. *J Biol Chem* **287**, 13877–13888.
- Wu L-J, Wu G, Akhavan Sharif MR, Baker A, Jia Y, Fahey FH, Luo HR, Feener EP & Clapham DE (2012). The voltage-gated proton channel Hv1 enhances brain damage from ischemic stroke. *Nat Neurosci* **15**, 565–573.

## Additional information

### Competing interests

The authors declare that they have no competing interests.

### Authors contribution

TKB, UBK, and TS conceived and designed the study and drafted the manuscript. TKB and TS co-ordinated the study and the experiments. TKB, DMF, NG, WB, AM, NDK, CB, DW, EK,



and TS designed experiments and acquired, analysed, and interpreted data. All authors approved the manuscript and revised the manuscript. All persons designated as authors qualify for authorship, and all those who qualify for authorship are listed.

### **Acknowledgements**

We would like to thank Sybille Wolf-Kümmeth for technical assistance. This work was supported by the German Research Foundation (grant BE5506/3-1 to TKB; SFB645 to TS and UBK).